Search for the electric dipole excitations to the $3s_{1/2}\otimes[2_1^+\otimes 3_1^-]$ multiplet in ^{117}Sn

J. Bryssinck,[1] L. Govor,[2] V. Yu. Ponomarev,[1,*] F. Bauwens,[1] O. Beck,[3] D. Belic,[3] P. von Brentano,[4] D. De Frenne,[1] C. Fransen,[4] R.-D. Herzberg,[4,†] E. Jacobs,[1] U. Kneissl,[3] H. Maser,[3] A. Nord,[3] N. Pietralla,[4] H. H. Pitz,[3] and V. Werner[4]

[1]*Vakgroep Subatomaire en Stralingsfysica, Universiteit Gent, Proeftuinstraat 86, 9000 Gent, Belgium*

[2]*Russian Scientific Centre ''Kurchatov Institute,'' Moscow, Russia*

[3]*Institut für Strahlenphysik, Universität Stuttgart, Stuttgart, Germany*

[4]*Institut für Kernphysik, Universität zu Köln, Köln, Germany*

(Received 4 February 2000; published 19 June 2000)

The odd-mass ^{117}Sn nucleus was investigated in nuclear resonance fluorescence experiments up to an end point energy of the incident photon spectrum of 4.1 MeV at the bremsstrahlung facility of the Stuttgart University. More than 50 mainly hitherto unknown levels were found. From the measurement of the scattering cross sections model independent absolute excitation strengths were extracted. The measured angular distributions suggested the spins of 11 excited levels. Quasiparticle phonon model calculations including a complete configuration space were performed for the first time for a heavy odd-mass spherical nucleus. These calculations give a clear insight in the fragmentation and distribution of the $E1$, $M1$, and $E2$ excitation strength in the low energy region. It is proven that the 1^- component of the two-phonon $[2_1^+\otimes 3_1^-]$ quintuplet built on top of the $1/2^+$ ground state is strongly fragmented. The theoretical calculations are consistent with the experimental data.

PACS number(s): 25.20.Dc, 23.20.−g, 21.10.Re, 21.60.−n

I. INTRODUCTION

Low-lying electric dipole excitations have been studied extensively in a variety of spherical [1] and deformed nuclei [2,3] over the last decade. A survey on the systematics of observed electric dipole excitations in the $A=130$–200 mass region is given in Ref. [4]. Systematic nuclear resonance fluorescence (NRF) experiments performed within the chains of the $N=82$ isotones [5] (^{138}Ba, ^{140}Ce, ^{142}Nd, and ^{144}Sm) and the $Z=50$ isotopes [6,7] ($^{116-124}$Sn) showed that the low-lying electric dipole strength $B(E1)\uparrow$ is mainly concentrated in the first $J^\pi=1_1^-$ state. Some uniform properties of these 1_1^- states were observed in both chains. Their excitation energies are lying close to the summed energies of the first quadrupole and octupole collective vibrational states and they are populated by an enhanced electric dipole excitation (two to three orders of magnitude larger than typical $E1$ transition strengths). Both arguments strongly suggest an underlying quadrupole-octupole coupled $[2_1^+\otimes 3_1^-]$ two-phonon structure. Indeed, a detailed microscopic study within the framework of the quasiparticle phonon model revealed a practically pure two-phonon $[2_1^+\otimes 3_1^-]_{1^-}$ configuration in the wave function of these 1_1^- states. The observed enhanced electric dipole strength of the ''forbidden'' $E1$ transitions can be reproduced from a consideration of the internal fermion structure of the phonons and taking into account a delicate destructive interference with the GDR 1^- one-phonons [7,8]. The most direct experimental proof for an underlying two-phonon structure can be obtained from a measurement of the decay pattern of the two-phonon states to their one-phonon components. This has been achieved up to now only in very few cases: ^{142}Nd, ^{144}Nd, and ^{144}Sm [9–13]. In each of these nuclei, the same $B(E2)$ strength could be measured in the $1_1^-\rightarrow 3_1^-$ as well as in the $2_1^+\rightarrow 0_{\text{g.s.}}^+$ decay consistent with a two-phonon picture. It is still a tough challenge to observe the other members of the $[2_1^+\otimes 3_1^-]$ two-phonon quintuplet as illustrated recently in Ref. [14].

As a natural extension of the systematic investigations on the even-even spherical nuclei, the question arises how the observed enhanced electric dipole excitation strength of the two-phonon $[2_1^+\otimes 3_1^-]_{1^-}$ state fragments over several levels of a particle two-phonon coupled multiplet in the odd-mass adjacent nuclei. In such a study, the experimental technique and the theoretical model should meet some requirements. In the first place, the experimental probe should be very selective in the excitation of levels because of the high level density in odd-mass nuclei. The number of the involved levels in the odd-mass nucleus increases drastically compared to the even-even neighboring nucleus: in the odd-mass nucleus levels with a spin equal J_0-1, J_0 and J_0+1 can be populated via dipole excitations from the ground state with spin J_0. Quadrupole transitions will excite levels with a spin between J_0-2 and J_0+2. The real photon probe is such a selective experimental tool. Using an intensive bremsstrahlung source only dipole and to a much lesser extent also electric quadrupole excitations will be induced. Secondly, the theoretical model should be able to distinguish between the degrees of freedom of the collective phonons and the additional particle degrees of freedom which open extra possible excitation channels and which have no counterparts in the even-even nuclei.

Electric dipole excitations to a particle-two-phonon multiplet were for the first time identified in ^{143}Nd [15]. In the

*Permanent address: Bogoliubov Laboratory of Theoretical Physics, Joint Institute of Nuclear Research, Dubna, Russia.

†Present address: Oliver Lodge Laboratory, University of Liverpool, Oxford Street, Liverpool L69 7ZE, UK.

energy region between 2.8 and 3.8 MeV, 13 levels were observed for which an underlying particle-two-phonon $f_{7/2}\otimes[2_1^+\otimes 3_1^-]$ structure was suggested. The observed fragmentation and $B(E1)\uparrow$ strength distribution could be reproduced in a phenomenological simple core coupling model based on quadrupole-quadrupole coupling [16]. Moreover, the summed experimental $B(E1)\uparrow$ strength between 2.8 and 3.8 MeV agrees within the statistical error with the known $B(E1)\uparrow$ strength of the two-phonon $[2_1^+\otimes 3_1^-]_{1^-}$ state in the neighboring even-mass ^{142}Nd nucleus. It was concluded that the unpaired neutron in its $f_{7/2}$ orbital, outside the closed major $N=82$ shell, couples extremely weakly to the two-phonon $[2_1^+\otimes 3_1^-]$ quintuplet and plays the role of a pure spectator. Later on, similar NRF-experiments performed on ^{139}La and ^{141}Pr [17] revealed also a large fragmentation of the electric dipole strength, but in both cases less than 40% of the two-phonon $B(E1)\uparrow$ strength in the neighboring even-mass ^{138}Ba, ^{140}Ce, and ^{142}Nd nuclei was observed. In ^{139}La and ^{141}Pr the odd proton in the partly filled shell couples more strongly to the two-phonon quintuplet. Intermediate cases have been observed in the open shell nuclei ^{113}Cd [18] and ^{133}Cs [19].

The odd-mass ^{117}Sn nucleus was chosen to investigate the fragmentation of the well-known two-phonon $B(E1)\uparrow$ strength from its even-mass neighbors ^{116}Sn and ^{118}Sn. The NRF technique was used for obvious reasons. In ^{117}Sn, the unpaired neutron is situated halfway between the major N = 50 and 82 shells. As an interesting property, the ground state spin $J_0^\pi=1/2^+$ limits the possible dipole excitations to levels with a spin $J=1/2$ or 3/2 and electric quadrupole excitations can only occur to states with a spin and parity $J^\pi=3/2^+$ and $5/2^+$. For the first time, calculations within the QPM are carried out in a complete configuration space for an odd-mass spherical nucleus. Our first results on the experimentally observed fragmentation and on the performed calculations were described in a previous paper [20]. In the present paper a comprehensive discussion of the experimental and theoretical aspects of our work will be presented.

II. EXPERIMENTAL METHOD AND SETUP

The nuclear resonance fluorescence technique, the resonant scattering of real photons off nuclei as described in many reviewing articles, e.g., [1,21,22], was applied to investigate the ^{117}Sn nucleus. The main advantages of this real photon probe consist of the highly selective excitation of levels, as pointed out in the Introduction, and the possibility of a completely model independent analysis of the data. The use of HP Ge detectors to detect the resonantly scattered photons, allows the observation of individual levels and the determination of their excitation energies E_x with a precision better than 1 keV. The total elastic scattering cross section I_S, energy integrated over a single resonance and integrated over the full solid angle equals [1]

$$I_S=g\left(\frac{\pi\hbar c}{E_x}\right)^2\frac{\Gamma_0^2}{\Gamma}, \tag{1}$$

with Γ_0 and Γ the ground state and total decay width and g a statistical factor depending on the ground state spin J_0 and the spin J of the excited level:

$$g=\frac{2J+1}{2J_0+1}. \tag{2}$$

In our experiments, the scattering cross sections of the observed levels in ^{117}Sn are determined relative to the ^{27}Al calibration standard. The spectral shape of the incoming bremsstrahlung flux is fitted using the Schiff formula for thin targets and the cross sections for the transitions in ^{117}Sn are extracted relatively to the cross sections of well-known transitions in ^{27}Al [23]. For even-even nuclei, the spin J of the excited level is easily obtained from the measured angular distribution of the resonantly scattered photons. A clear distinction between dipole and quadrupole transitions can be made by comparing the observed γ intensities at the scattering angles of 90° and 127° [1]. However, for odd-mass nuclei the extraction of limited spin information is only possible for nuclei as ^{117}Sn with a ground state spin J_0 of 1/2 [18]. Higher half integer ground state spins lead to nearly isotropic angular distributions. From an evaluation of the angular distribution function W for the involved spin sequence, scattering angle and multipole mixing ratio δ, the following results are obtained:

$\frac{1}{2}\rightarrow\frac{1}{2}\rightarrow\frac{1}{2}$

$$\frac{W(90°)}{W(127°)}=1,\quad \frac{W(90°)}{W(150°)}=1, \tag{3}$$

$\frac{1}{2}\rightarrow\frac{3}{2}\rightarrow\frac{1}{2}$

$$\frac{W(90°)}{W(127°)}=0.866,\quad \frac{W(90°)}{W(150°)}=0.757,\quad \delta=0,\pm\infty, \tag{4}$$

$\frac{1}{2}\rightarrow\frac{5}{2}\rightarrow\frac{1}{2}$

$$\frac{W(90°)}{W(127°)}=1.168,\quad \frac{W(90°)}{W(150°)}=0.842,\quad \delta=0. \tag{5}$$

The scattering angles correspond to those used in our experiments. The angular distribution functions W are independent of the parity of the excited level. In Fig. 1 the expected angular correlation function ratios are shown in a $W(90°)/W(150°)$ versus $W(90°)/W(127°)$ plot for different values of the mixing ratio δ and for the three possible induced spin sequences. A level with spin 1/2 can only be excited from the ground state via a dipole transition and hence no mixing of multipolarities is possible in a 1/2-1/2-1/2 spin cascade. Such a cascade has an isotropic angular distribution function W. The square in Fig. 1 represents the unique location in this figure where 1/2-1/2-1/2 spin sequences can be found. In the case of a 1/2-3/2-1/2 spin sequence, the intensity ratios $W(90°)/W(127°)$ and $W(90°)/W(150°)$ are strongly influenced by the mixing ratio δ. This results in the solid line in Fig. 1. For pure $E1$ and $M1$ transitions to the 3/2 level, corresponding to a mixing ratio δ equal 0, or for pure $E2$ transitions, with a mixing

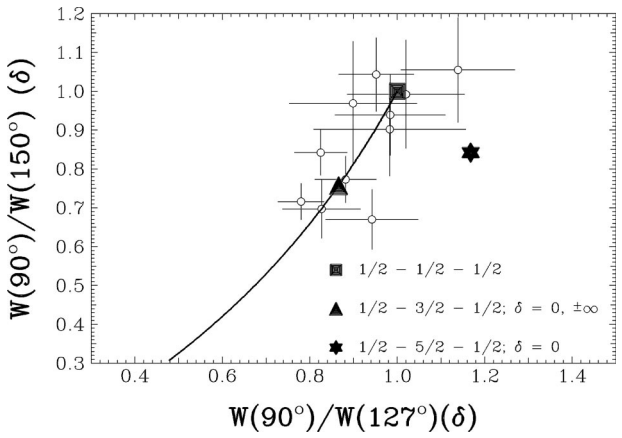

FIG. 1. Observed angular distribution ratios $W(90°)/W(150°)$ versus $W(90°)/(127°)$ (open points with error bars). The square represents the unique location for 1/2-1/2-1/2 spin sequences. Pure $E1$, $M1$, or $E2$ transitions in a 1/2-3/2-1/2 spin sequence are marked with the triangle. $E1$ and mixed $M1/E2$ transitions ($\delta \neq 0, \pm\infty$) in this spin sequence are located on the solid line. The star corresponds to a pure $E2$ transition in a 1/2-5/2-1/2 spin sequence.

ratio δ equal $\pm\infty$, the same two values for the ratios $W(90°)/W(127°)$ and $W(90°)/W(150°)$ are obtained [see Eq. (4)]. This is represented by the triangle in Fig. 1. For a 1/2-5/2-1/2 spin sequence, only pure $E2$ excitations to the 5/2 level are observed in our NRF experiments. The star in Fig. 1 represents the expected position of these 1/2-5/2-1/2 spin sequences. Experimental points are included in Fig. 1. They will be discussed in Sec. III. For the strongest transitions observed with a high statistical precision, the experimental uncertainties on the ratios $W(90°)/W(127°)$ and $W(90°)/(150°)$ will be small enough to suggest the induced half integer spin sequence. In most cases the statistical accuracy will not allow to determine the spin sequence and hence the statistical spin factor g cannot be determined.

Compton polarimetry [24] and the scattering of linearly polarized off-axis bremsstrahlung [25,26] represent two useful techniques to determine the parities of the excited levels in even-even nuclei [1]. For odd-mass nuclei, the measured azimuthal asymmetry of the resonantly scattered photons and their polarization will nearly vanish because of the half integer spin sequences and it will strongly depend on the mixing ratio δ. The lower statistics in these experiments do not allow to distinguish between the different possible cases. For a further analysis of the data, it will be assumed that all observed levels are populated via pure electric dipole excitations and that they do not have any decay branchings (unless observed experimentally) to intermediate lower-lying levels ($\Gamma_0/\Gamma = 1$). This assumption, imposed because of the lack of experimental information on the spin and parities of the excited levels, is justified by the fact that in general $E1$ transitions have higher transition probabilities than $M1$ or $E2$ transitions. It should however be remarked that this assumption contains some risk as will become clear further in this paper from the results of theoretical calculations. Under the above assumption, the product of the ground state transition width and the spin factor g can immediately be extracted from the measured scattering cross section I_S [Eq. (1)] and the reduced electric dipole excitation probability is given by

$$B(E1)\uparrow = \frac{2.866}{3}\frac{g\cdot\Gamma_0}{E_x^3}(10^{-3}\ \ e^2\,\mathrm{fm}^2), \qquad (6)$$

with the ground state transition width Γ_0 in meV and the excitation energy E_x in MeV. The deduced $B(E1)\uparrow$ strength in our NRF experiments includes automatically the statistical factor g and hence can immediately be compared with the observed $B(E1)\uparrow$ strength in other nuclei or calculated from theoretical models.

The experiments were performed at the NRF-facility of the 4.3 MV Dynamitron accelerator of the Stuttgart University. The energy of the electron beam was 4.1 MeV and the beam current was limited to about 250 μA due to the thermal capacity of the bremsstrahlung production target and to avoid too high count rates in the detectors. A setup consisting of 3 HP Ge detectors, installed at scattering angles of 90°, 127°, and 150° each with an efficiency ϵ of 100% [relative to a 3×3 in.^{2} NaI(Tl) detector], was used to measure the total elastic scattering cross sections of the levels in ^{117}Sn. These HP Ge detectors allow to detect the resonantly scattered photons with a high sensitivity and a very good energy resolution. Two metallic Sn disks with a diameter of 1 cm, a total weight of 1.649 g, and an isotopic enrichment of 92.10% in ^{117}Sn were irradiated during five days. Two ^{27}Al disks with a total amount of 0.780 g were alternated with the two ^{117}Sn disks for calibration purposes.

III. RESULTS

Part of the recorded ^{117}Sn (γ,γ') spectrum ($2.6 \leqslant E_\gamma \leqslant 3.6$ MeV) is shown in Fig. 2 together with the spectra of its even-even ^{116}Sn and ^{118}Sn neighbors. In our previous studies on ^{116}Sn and ^{118}Sn [7], we found that the $E1$ strength in this energy region below 4 MeV is mostly concentrated in the two-phonon $[2_1^+\otimes 3_1^-]_{1^-}$ state. In the spectra of the even-even nuclei, the dominating peak at an energy of about 3.3 MeV corresponds to the deexcitation of this two-phonon 1^- state into the ground state. In comparison to the spectra of the even-even Sn nuclei, the ^{117}Sn spectrum contains a lot of γ transitions superimposed on the smooth background in the vicinity of the two-phonon 1^- states. The peaks stemming from the deexcitation of the two-phonon $[2_1^+\otimes 3_1^-]_{1^-}$ states in ^{116,118,120}Sn have also been observed in the spectrum due to the small admixtures of 0.86%, 5.81%, and 0.76% in the target. In Fig. 2(b) only the peak for ^{118}Sn can be clearly observed due to the scale used. All observed γ transitions in ^{117}Sn are listed in Table I with the corresponding level excitation energies, the measured total elastic scattering cross sections I_S, the extracted transition width ratios $g\cdot(\Gamma_0^2/\Gamma)$ (depending on the statistical spin-factor g) and deduced electric excitation probabilities $B(E1)\uparrow$. The total elastic scattering cross sections has been determined from a summed spectrum over the three scattering angles. The three HP Ge-detectors have nearly the same efficiency and in the summed spectra the angular dependence of the transition intensity on

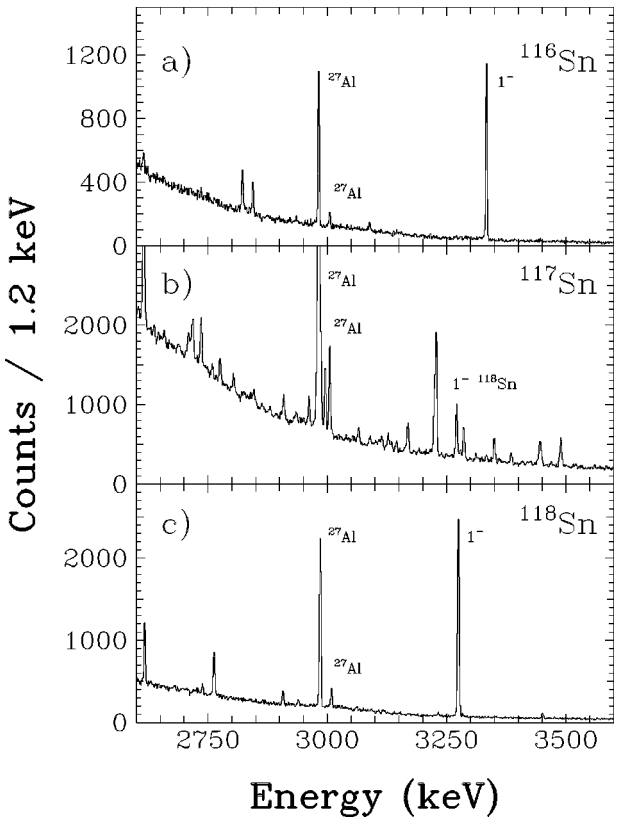

FIG. 2. Photon scattering spectra of the odd-mass ^{117}Sn (summed spectrum) inserted between those of the even-even ^{116}Sn and ^{118}Sn nuclei (at a scattering angle of 127°), all taken with an end point energy of 4.1 MeV.

the possible spin cascade is averaged out. This method allows us to observe also some weaker lines.

In some cases, the observed angular distribution ratios provide an indication of the spin J of the photoexcited levels. These results are summarized in Table II. In the first column the energies of these levels are given. In the next columns the observed angular distribution ratios $W(90°)/W(127°)$ and $W(90°)/W(150°)$ and the suggested spin are presented. The experimentally observed angular distribution ratios $W(90°)/W(150°)$ versus $W(90°)/(127°)$ are included in Fig. 1 (open points with error bars). Two groups of γ transitions can clearly be observed. For a first group of 5 levels, located around the triangle, a probable spin assignment of 3/2 can be given. A second group of 6 levels can be found around the square. Here an assignment of 1/2 (3/2) can be given. We prefer $J=1/2$ for these states because we suppose that strong transitions should have an $E1$ character. These $E1$ transitions have an isotropic distribution only for excited states with $J=1/2$. However we cannot exclude $J=3/2$ (negative or positive parity) as transitions with a mixing ratio δ around -3.73 or 0.27 also lead to an isotropic distribution. All the spins given in Table II were assigned at least at a statistical significance level of 1σ. Under these conditions, no levels with a spin of 5/2 were found.

Five of the observed γ transitions are probably due to inelastic deexcitations of a level to the well-known first $3/2^+$ state in ^{117}Sn at 158.562(12) keV [27]. They are summarized in Table III. In this table the level excitation energies E_x, the energies E_γ of the deexciting γ transitions, the relative γ intensities I_γ, the ground state transition widths $g\cdot\Gamma_0$, and reduced electric dipole excitation probabilities corrected for the observed inelastic decays, are given. All levels are included for which holds

$$E_i-(E_x-E_{158})<\Delta E, \tag{7}$$

with

$$\Delta E=\sqrt{(\Delta E_x)^2+(\Delta E_i)^2+(\Delta E_{158})^2} \tag{8}$$

and E_x, E_i, E_{158}, and ΔE_x, ΔE_i, ΔE_{158} the excitation energies of the level, the energy of the inelastic γ transition and the first $3/2^+$ state and their respective uncertainties. Using the above mentioned rule for detecting inelastic decays two other candidates were found. The γ ray with the energy of 3560.5 keV can be due to an inelastic transition of one line from the multiplet at 3719.8 keV to the first $3/2^+$ state. Also the γ ray with the energy of 2986.7 keV fits into the energy relation with the observed level at 3144.9 keV. However, when this γ ray is seen as completely inelastic, an unreasonable low branching ratio Γ_0/Γ of 12% for the 3144.9 keV level is obtained. Both cases are not considered in Table III. Certainty about the observed probable inelastic γ transitions requires time coincidence or excitation function measurements. With the above mentioned method, our experimental results show no further candidates for inelastic transitions to other excited levels.

IV. DISCUSSION

According to the phenomenological core coupling model, the level scheme for ^{117}Sn can be obtained from the coupling of the unpaired $3s_{1/2}$ neutron to the ^{116}Sn core. This is schematically shown in Fig. 3. Each level in ^{116}Sn (except for $J=0$ levels) gives rise to two new levels due to the spin 1/2 of the unpaired neutron. The low-lying level scheme of ^{116}Sn is dominated by the strong quadrupole (2^+) and octupole (3^-) vibrational states, typical for a spherical semimagic nucleus. The coupling of the $3s_{1/2}$ neutron to the first 2^+ state in ^{116}Sn results in two new levels $[3s_{1/2}\otimes 2_1^+]_{3/2^+}$ and $[3s_{1/2}\otimes 2_1^+]_{5/2^+}$ which can be excited in NRF via $M1$ and $E2$ transitions (solid lines in Fig. 3). The similar doublet consisting of the $[3s_{1/2}\otimes 3_1^-]_{5/2^-}$ and $[3s_{1/2}\otimes 3_1^-]_{7/2^-}$ states requires $M2$ and $E3$ excitations which are not observable in NRF (dashed lines). The main aim of our NRF experiments was to search for levels belonging to the $3s_{1/2}\otimes[2_1^+\otimes 3_1^-]$ multiplet which can be populated via electric dipole transitions. When the quadrupole-octupole coupled two-phonon quintuplet is built on top of the $1/2^+$ ground state, a multiplet of 10 negative parity states is obtained of which 3 levels can be excited via $E1$ transitions (solid lines in Fig. 3). In this simple model, these three transitions carry the complete $B(E1)\uparrow$ strength. In Fig. 4(b) the obtained total scattering cross sections I_S for the photo-excited levels in ^{117}Sn (with exclusion of the lines which are probable due to inelastic scattering given in Table III) and in its even-even neighbors

TABLE I. Properties of the observed levels in ^{117}Sn. The excitation energies, integrated cross sections I_S, transition width ratios $g \cdot \Gamma_0^2/\Gamma$, and the excitation probabilities $B(E1)\uparrow$ are given.

Energy (keV)	I_S (eV b)	$g\frac{\Gamma_0^2}{\Gamma}$ (meV)	$B(E1)\uparrow$ [a] (10^{-3} e^2 fm^2)
1447.2 (4)	2.31 (40)	1.26 (22)	0.398 (68)
1510.1 (3)	4.12 (48)	2.45 (29)	0.679 (80)
2048.2 (3)	6.20 (49)	6.77 (54)	0.752 (60)
2128.6 (4)	1.05 (22)	1.24 (25)	0.123 (25)
2280.4 (6)	0.45 (16)	0.61 (22)	0.049 (18)
2304.6 (5)	0.73 (18)	1.01 (25)	0.079 (20)
2356.7 (8)[b]	0.80 (25)	1.15 (36)	0.084 (27)
2367.3 (2)	7.86 (55)	11.46 (80)	0.825 (58)
2415.9 (3)	1.86 (23)	2.82 (35)	0.191 (24)
2515.8 (5)	0.72 (17)	1.18 (28)	0.071 (17)
2590.2 (5)	1.00 (23)	1.75 (40)	0.096 (22)
2709.1 (5)	1.46 (22)	2.80 (42)	0.134 (20)
2718.2 (4)	1.74 (43)	3.34 (82)	0.159 (39)
2775.2 (4)	1.02 (19)	2.04 (37)	0.091 (17)
2803.4 (5)[b]	1.19 (20)	2.43 (42)	0.105 (18)
2864.1(11)	0.57 (21)	1.21 (45)	0.049 (18)
2879.8 (9)	0.58 (20)	1.25 (42)	0.050 (17)
2908.5 (4)	2.15 (28)	4.73 (62)	0.184 (24)
2961.9 (4)	2.66 (28)	6.08 (63)	0.224 (23)
2986.7 (3)	7.28 (85)	16.89 (197)	0.606 (71)
2995.7 (3)	5.48 (41)	12.80 (96)	0.455 (34)
3065.7 (5)[b]	1.53 (22)	3.74 (55)	0.124 (18)
3100.8 (7)	0.76 (15)	1.91 (38)	0.061 (12)
3108.2 (7)	0.83 (17)	2.08 (43)	0.066 (14)
3127.8 (4)[b]	1.75 (21)	4.45 (53)	0.139 (17)
3134.3 (6)	0.96 (17)	2.46 (43)	0.076 (13)
3144.9 (5)	1.11 (18)	2.86 (45)	0.088 (14)
3169.1 (4)	3.36 (32)	8.78 (83)	0.264 (25)
3224.6(11)	5.71 (51)	15.45 (137)	0.440 (39)
3228.2 (7)	12.80 (91)	34.71 (247)	0.986 (71)
3286.0 (4)	3.57 (35)	10.05 (97)	0.284 (26)
3349.9 (3)	3.25 (31)	9.50 (90)	0.242 (23)
3360.1 (8)	0.55 (20)	1.60 (59)	0.040 (15)
3385.4 (4)	1.39 (21)	4.15 (63)	0.102 (16)
3408.5 (9)	0.52 (19)	1.57 (58)	0.038 (14)
3425.8 (9)	0.60 (25)	1.84 (75)	0.044 (18)
3468.8 (6)	0.47 (16)	1.47 (49)	0.034 (11)
3489.6 (3)	5.46 (48)	17.31 (151)	0.389 (34)
3520.4 (7)	0.53 (20)	1.70 (64)	0.037 (14)
3560.5 (6)	0.54 (16)	1.79 (53)	0.038 (11)
3719.8 (7)[c]	3.16 (45)	11.38 (163)	0.211 (30)
3749.4 (4)	2.08 (34)	7.62 (123)	0.138 (22)
3761.4 (8)[b]	0.90 (32)	3.32 (117)	0.060 (21)
3773.3(13)	0.91 (39)	3.37 (144)	0.060 (26)
3788.3 (7)	1.57 (36)	5.87 (133)	0.103 (24)
3871.3 (4)	5.05 (65)	19.71 (255)	0.325 (42)
3883.2 (4)	3.58 (53)	14.06 (207)	0.229 (34)
3900.2 (6)	1.09 (29)	4.33 (117)	0.070 (19)
3920.1 (7)	1.45 (40)	5.79 (158)	0.092 (25)
3930.4 (5)	1.12 (29)	4.51 (117)	0.071 (19)
3949.8 (16)	3.21 (137)	13.03 (558)	0.202 (87)
3980.9 (5)	3.47 (68)	14.31 (280)	0.217 (43)
3994.0 (6)	1.73 (46)	7.17 (189)	0.108 (29)
4013.6 (6)	2.54 (77)	10.65 (324)	0.157 (48)
4027.8 (4)	6.56 (129)	27.70 (544)	0.405 (80)
4043.6 (7)	3.94 (113)	16.78 (482)	0.242 (70)

[a]Assuming electric dipole excitations.
[b]The γ transition might be due to an inelastic decay of a higher-lying level; see Table III.
[c]Multiplet.

^{116}Sn [Fig. 4(a)] and ^{118}Sn [Fig. 4(d)] are plotted. The total scattering cross section for the excitation of the two-phonon $[2_1^+ \otimes 3_1^-]$ states in ^{116}Sn and ^{118}Sn has been reduced by a factor of 3. A strong fragmentation of the strength has been observed in ^{117}Sn compared to its even-even neighbors. It is already clear from the observed fragmentation of the strength that a phenomenological core coupling model, which was successful in describing the observed strength in ^{143}Nd, will be insufficient in our case. Due to a lack of spin and parity information of the photo-excited levels in ^{117}Sn in our NRF experiment and due to a lack of experimental data from other investigations [27], we need to turn to a more elaborated theoretical interpretation to get more insight.

A. QPM formalism for odd-mass nuclei

The quasiparticle phonon model (QPM) was already successful in describing collective properties in even-even mass nuclei [28]. Recently, the QPM has been applied to describe

TABLE II. Suggested spin assignments for some levels in ^{117}Sn. For each level, the observed angular correlation ratios $W(90°)/W(127°)$ and $W(90°)/W(150°)$ are given. The last column contains the suggested spin.

Energy (keV)	$\frac{W(90°)}{W(127°)}$	$\frac{W(90°)}{W(150°)}$	J
2048.2	0.952 (86)	1.043 (95)	$\frac{1}{2}$ ($\frac{3}{2}$)
2367.3	0.780 (53)	0.716 (47)	$\frac{3}{2}$
2986.7	0.983 (174)	0.902 (120)	$\frac{1}{2}$ ($\frac{3}{2}$)
2995.7	0.882 (70)	0.773 (60)	$\frac{3}{2}$
3169.1	0.942 (106)	0.670 (77)	$\frac{3}{2}$
3224.6	0.984 (126)	0.939 (104)	$\frac{1}{2}$ ($\frac{3}{2}$)
3228.2	0.825 (60)	0.842 (58)	$\frac{3}{2}$
3286.0	1.139 (130)	1.055 (135)	$\frac{1}{2}$ ($\frac{3}{2}$)
3349.9	1.020 (134)	0.992 (139)	$\frac{1}{2}$ ($\frac{3}{2}$)
3489.6	0.827 (89)	0.697 (75)	$\frac{3}{2}$
3871.3	0.899 (146)	0.969 (159)	$\frac{1}{2}$ ($\frac{3}{2}$)

TABLE III. Levels with probable inelastic transitions to the 158.562 keV ($3/2^+$) level in ^{117}Sn. Columns two and three contain for each level the energy of the observed γ rays and the γ intensity. The given ground state decay widths $g\cdot\Gamma_0$ and the $B(E1)\uparrow$ strengths are corrected for the possible inelastic transitions.

E_x (keV)	E_γ (keV)	I_γ	$g\cdot\Gamma_0$ (meV)	$B(E1)\uparrow$ (10^{-3} e^2 fm^2)
2515.8 (5)	2515.8 (5)	100.0	2.7 (8)	0.162 (49)
	2356.7 (8)	127.6 (435)		
2961.9 (4)	2961.9 (4)	100.0	9.2 (11)	0.338 (39)
	2803.4 (5)	51.3 (78)		
3224.6 (11)	3224.6 (11)	100.0	20.3 (6)	0.577 (17)
	3065.7 (5)	31.2 (37)		
3286.0 (4)	3286.0 (4)	100.0	16.3 (16)	0.439 (43)
	3127.8 (4)	54.5 (53)		
3920.1 (7)	3920.1 (7)	100.0	11.4 (38)	0.180 (60)
	3761.4 (8)	96.0 (375)		

the position and the $E1$ excitation probability of the lowest 1^- state in the even-even $^{116-124}$Sn isotopes [7]. This state has a two-phonon character with a contribution of the $[2_1^+\otimes 3_1^-]_{1^-}$ configuration of 96–99 %. For odd-mass nuclei, this model was used to describe the fragmentation of deep-lying hole and high-lying particle states [29,30] and the photoproduction of isomers [31–33]. It has already been applied to calculate the absolute amount of strength in ^{115}In [34], but until now it has not been extended to describe and understand the high fragmentation of the strength and the distribution of the $B(E1)\uparrow$, $B(M1)\uparrow$, and $B(E2)\uparrow$ strength in the energy region below 4 MeV.

General ideas about the QPM and its formalism to describe the excited states in odd-mass spherical nuclei with a wave function which includes ''quasiparticle$\otimes N$-phonon'' configurations, with $N=0,1,2$, are presented in review articles [29,30]. It is extended here by including ''quasiparticle $\otimes$ three-phonon'' configurations as well. A Woods-Saxon potential is used in the QPM as an average field for protons and neutrons. Phonons of different multipolarities and parities are obtained by solving the RPA equations with a separable form of the residual interaction including a Bohr-Mottelson form factor. The single-particle spectrum and phonon basis are fixed from calculations in the neighboring

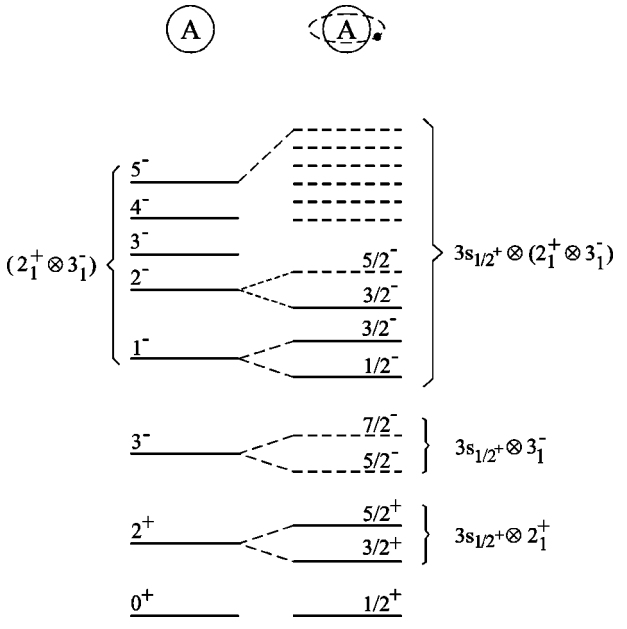

FIG. 3. Schematic level schemes for the odd-mass ^{117}Sn nucleus and the even-even core nucleus ^{116}Sn. The level scheme for ^{117}Sn can be obtained in a phenomenological simple core coupling model by coupling the $3s_{1/2}$ neutron to the even-even ^{116}Sn neighbor.

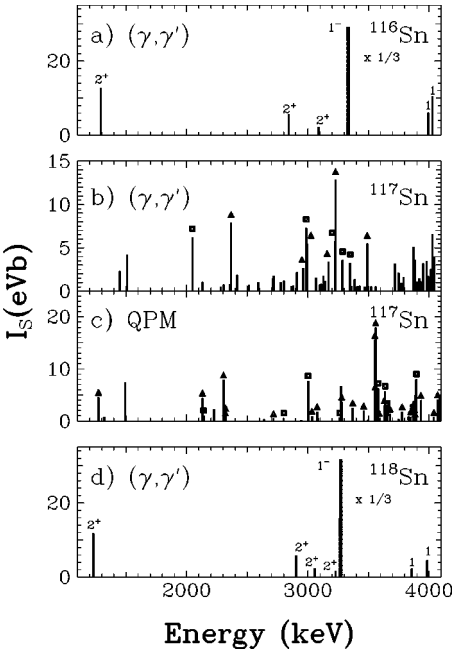

FIG. 4. Total integrated photon scattering cross sections I_S observed in ^{117}Sn (b) centered between those observed in its even-even neighbors ^{116}Sn (a) and ^{118}Sn (d) [37]. The integrated elastic photon scattering cross sections calculated within the QPM are included in panel (c) for comparison. The lines marked by a triangle correspond to levels with a 3/2 spin. The squares represent levels with a 1/2 (3/2) spin.

even-even nuclear core, i.e., in ^{116}Sn [7] when the ^{117}Sn nucleus is considered.

In our present calculations the wave functions of the ground state and the excited states are mixtures of different ''quasiparticle$\otimes N$-phonon'' ($[qp\otimes Nph]$) configurations, where $N=0,1,2,3$:

$$\Psi^{\nu}(JM)=\left\{ C^{\nu}(J)\alpha^{+}_{JM}+\sum_{j\beta_1} S^{\nu}_{j\beta_1}(J)[\alpha^{+}_{j}Q^{+}_{\beta_1}]_{JM}+\sum_{j\beta_1\beta_2}\frac{D^{\nu}_{j\beta_1\beta_2}(J)[\alpha^{+}_{j}Q^{+}_{\beta_1}Q^{+}_{\beta_2}]_{JM}}{\sqrt{1+\delta_{\beta_1\beta_2}}} \right.$$
$$\left. +\sum_{j\beta_1\beta_2\beta_3}\frac{T^{\nu}_{j\beta_1\beta_2\beta_3}(J)[\alpha^{+}_{j}Q^{+}_{\beta_1}Q^{+}_{\beta_2}Q^{+}_{\beta_3}]_{JM}}{\sqrt{1+\delta_{\beta_1\beta_2}+\delta_{\beta_1\beta_3}+\delta_{\beta_2\beta_3}+2\delta_{\beta_1\beta_2\beta_3}}}\right\}|\rangle_{\rm g.s.}, \tag{9}$$

where the coefficients C, S, D, and T describe a contribution of each configuration to a norm of the wave function. We use the following notations α^{+} and Q^{+} for the coupling between the creation operators of quasiparticles and phonons:

$$[\alpha^{+}_{j}Q^{+}_{\lambda i}]_{JM}=\sum_{m\mu}C^{JM}_{jm\lambda\mu}\alpha^{+}_{jm}Q^{+}_{\lambda\mu i},$$

$$[\alpha^{+}_{j}Q^{+}_{\beta_1}Q^{+}_{\beta_2}Q^{+}_{\beta_3}]_{JM}=\sum_{\lambda_1\lambda_2}[\alpha^{+}_{j}[Q^{+}_{\beta_1}[Q^{+}_{\beta_2}Q^{+}_{\beta_3}]_{\lambda_1}]_{\lambda_2}]_{JM},$$

$$[Q^{+}_{\lambda_1 i_1}Q^{+}_{\lambda_2 i_2}]_{\lambda\mu}=\sum_{\mu_1\mu_2}C^{\lambda\mu}_{\lambda_1\mu_1\lambda_2\mu_2}Q^{+}_{\lambda_1\mu_1 i_1}Q^{+}_{\lambda_2\mu_2 i_2}, \tag{10}$$

where C are Clebsh-Gordon coefficients. Quasiparticles are characterized by their shell quantum numbers $jm\equiv|nljm\rangle$ with a half integer value of the total angular momenta j. They are the result of a Bogoliubov transformation from particle creation (annihilation) a^{+}_{jm} (a_{jm}) operators:

$$a^{+}_{jm}=u_j\alpha^{+}_{jm}+(-1)^{j-m}v_j\alpha_{j-m}. \tag{11}$$

The quasiparticle energy spectrum and the occupation number coefficients u_j and v_j in Eq. (11) are obtained in the QPM by solving the BCS equations separately for neutrons and protons.

Phonons with quantum numbers $\beta\equiv|\lambda\mu i\rangle$ are linear superpositions of two-quasiparticle configurations:

$$Q^{+}_{\lambda\mu i}=\frac{1}{2}\sum_{\tau}^{n,p}\sum_{jj'}\{\psi^{\lambda i}_{jj'}[\alpha^{+}_{j}\alpha^{+}_{j'}]_{\lambda\mu}$$
$$-(-1)^{\lambda-\mu}\varphi^{\lambda i}_{jj'}[\alpha_{j'}\alpha_{j}]_{\lambda-\mu}\}. \tag{12}$$

A spectrum of phonon excitations is obtained by solving the RPA equations for each multipolarity λ which is an integer value. The RPA equations also yield forward (backward) $\psi^{\lambda i}_{jj'}$ ($\varphi^{\lambda i}_{jj'}$) amplitudes in definition (12):

$$\begin{pmatrix}\psi\\ \varphi\end{pmatrix}^{\lambda i}_{jj'}(\tau)=\frac{1}{\sqrt{\mathcal{Y}^{\lambda i}_{\tau}}}\frac{f^{\lambda}_{jj'}(\tau)(u_jv_{j'}+u_{j'}v_j)}{\varepsilon_j+\varepsilon_{j'}\mp\omega_{\lambda i}}, \tag{13}$$

where ε_j is a quasiparticle energy, $\omega_{\lambda i}$ is the energy needed for the excitation of an one-phonon configuration, $f^{\lambda}_{jj'}$ is a reduced single-particle matrix element of residual forces, and the value $\mathcal{Y}^{\lambda i}_{\tau}$ is determined from a normalization condition for the phonon operators:

$$\langle|Q_{\lambda\mu i}Q^{+}_{\lambda\mu i}|\rangle_{ph}=\sum_{\tau}^{n,p}\sum_{jj'}\{(\psi^{\lambda i}_{jj'})^2-(\varphi^{\lambda i}_{jj'})^2\}=1. \tag{14}$$

The phonon's index i is used to distinguish between phonon excitations with the same multipolarity but with a difference in energy and structure. The RPA equations yield both, collective- (e.g., 2^{+}_{1} and 3^{-}_{1}), and weakly-collective phonons. The latter correspond to phonons for which some specific two-quasiparticle configuration is dominant in Eq. (12) while for other configurations $\psi^{\lambda i}_{jj'},\varphi^{\lambda i}_{jj'}\approx 0$.

When the second, third, etc., terms in the wave function of Eq. (9) are considered, phonon excitations of the core couple to a quasiparticle at any level of the average field, not only at the ones with the quantum numbers J^{π} as for a pure quasiparticle configuration. It is only necessary that all configurations in Eq. (9) have the same total spin and parity. To achieve a correct position of the $[qp\otimes 2ph]$ configurations, in which we are especially interested in these studies, $[qp\otimes 3ph]$ configurations are important. The excitation energies and the contribution of the different components from the configuration space to the structure of each excited state [i.e., coefficients C, S, D, and T in Eq. (9)] are obtained by a diagonalization of the model Hamiltonian on a set of employed wave functions. The coupling matrix elements between the different configurations in the wave functions of Eq. (9) in odd-mass nuclei are calculated on a microscopic footing, making use of the internal fermion structure of the phonons and the model Hamiltonian. For example, the interaction matrix element between the $[qp\otimes 1ph]$ and the $[qp\otimes 2ph]$ configurations has the form (see Ref. [30])

$$\langle[\alpha_{jm}Q_{\lambda\mu i}]_{JM}|H|[\alpha^{+}_{j'm'}[Q^{+}_{\lambda_1\mu_1 i_1}Q^{+}_{\lambda_2\mu_2 i_2}]_{IM'}]_{JM}\rangle$$
$$=\delta_{jj'}\delta_{\lambda I}U^{\lambda_2 i_2}_{\lambda_1 i_1}(\lambda i)-(-)^{j'+\lambda+I}2\sqrt{(2j+1)(2I+1)}$$
$$\times\left[(-)^{\lambda_1}\delta_{\lambda\lambda_1}\begin{Bmatrix}\lambda_2 & \lambda_1 & I\\ J & j & j'\end{Bmatrix}\Gamma(jj'\lambda_2 i_2)\right.$$
$$\left.+(-)^{\lambda_2}\delta_{\lambda\lambda_2}\begin{Bmatrix}\lambda_1 & \lambda_2 & I\\ J & j & j'\end{Bmatrix}\Gamma(jj'\lambda_1 i_1)\right], \tag{15}$$

where H is a model Hamiltonian, $U^{\lambda_2 i_2}_{\lambda_1 i_1}(\lambda i)$ is an interaction matrix element between one- and two-phonon configurations in the neighboring even-mass nucleus (U is a complex function of phonon's amplitudes ψ and φ and $f^{\lambda}_{jj'}$; its explicit form can be found in Ref. [35]) and Γ is an interaction matrix element between quasiparticle α^{+}_{JM} and quasiparticle-phonon $[\alpha^{+}_{jm}Q^{+}_{\lambda\mu i}]_{JM}$ configurations. It is equal to

$$\Gamma(Jj\lambda i)=\sqrt{\frac{2\lambda+1}{2J+1}}\,\frac{f^{\lambda}_{Jj}(u_J u_j - v_j v_J)}{\sqrt{\mathcal{Y}^{\lambda i}_{\tau}}}. \tag{16}$$

Equations (15) and (16) are obtained by applying the exact commutation relations between the phonon and quasiparticle operators:

$$[\alpha_{jm},Q^{+}_{\lambda\mu i}]_{-}=\sum_{j'm'}\psi^{\lambda i}_{jj'}C^{\lambda\mu}_{jmj'm'}\alpha^{+}_{j'm'},$$
$$[\alpha^{+}_{jm},Q^{+}_{\lambda\mu i}]_{-}=(-1)^{\lambda-\mu}\sum_{j'm'}\varphi^{\lambda i}_{jj'}C^{\lambda-\mu}_{jmj'm'}\alpha_{j'm'}. \tag{17}$$

The exact commutation relations between the phonon operators $Q_{\lambda\mu i}$ and $Q^{+}_{\lambda'\mu'i'}$

$$\begin{aligned}[Q_{\lambda\mu i},Q^{+}_{\lambda'\mu'i'}]_{-}&=\delta_{\lambda\lambda'}\delta_{\mu\mu'}\delta_{ii'}\\&-\sum_{\substack{jj'j_2\\mm'm_2}}\alpha^{+}_{jm}\alpha_{j'm'}\{\psi^{\lambda i}_{j'j_2}\psi^{\lambda' i'}_{jj_2}C^{\lambda\mu}_{j'm'j_2m_2}\\&\times C^{\lambda'\mu'}_{jmj_2m_2}-(-)^{\lambda+\lambda'+\mu+\mu'}\varphi^{\lambda i}_{jj_2}\varphi^{\lambda' i'}_{j'j_2}\\&\times C^{\lambda-\mu}_{jmj_2m_2}C^{\lambda'-\mu'}_{j'm'j_2m_2}\}\end{aligned} \tag{18}$$

are used to calculate the interaction matrix elements U in even-even nuclei.

The interaction matrix elements between the $[qp\otimes 2ph]$ and the $[qp\otimes 3ph]$ configurations have a structure similar to Eq. (15). We do not provide them here because of their complexity. But even Eq. (15) shows that an unpaired quasiparticle does not behave as a spectator but modifies the interaction between the complex configurations compared to an even-mass nucleus (see second term in this equation). This takes place because the phonons possess an internal fermion structure and the matrix elements Γ correspond to an interaction between an unpaired quasiparticle and the two-quasiparticle configurations composing the phonon operator.

It should be pointed out that in the present approach interaction matrix elements are calculated in first order perturbation theory. This means that any $[qp\otimes Nph]$ configuration interacts with the $[qp\otimes(N\pm 1)ph])$ ones, but its coupling to $[qp\otimes(N\pm 2)ph]$ configurations is not included in this theoretical treatment. The omitted couplings have nonvanishing interaction matrix elements only in second order perturbation theory. They are much smaller than the ones taken into account and they are excluded from our consideration for technical reasons. An interaction with other $[qp\otimes Nph]$ configurations is taken into account while treating the Pauli principle corrections. In a calculation of the self-energy of the complex configurations we employ a model Hamiltonian written in terms of quasiparticle operators and exact commutation relations (17) and (18) between quasiparticle and phonon operators. In this case, we obtain a ''Pauli shift correction'' for the energy of a complex configuration from the sum of the energies of its constituents. Also, when considering complex configurations their internal fermion structure is analyzed and the ones which violate the Pauli principle are excluded from the configuration space. Pauli principle corrections have been treated in a diagonal approximation (see Ref. [29] for details).

In the actual calculations, the phonon basis includes the phonons with multipolarity and parity $\lambda^{\pi}=1^{\pm},2^{+},3^{-}$, and 4^{+}. Several low-energy phonons of each multipolarity are included in the model space. The most important ones are the first collective 2^{+}, 3^{-}, and 4^{+} phonons and the ones which form the giant dipole resonance (GDR). Noncollective low-lying phonons of an unnatural parity and natural parity phonons of higher multipolarities are of a marginal importance. To make realistic calculations possible one has to truncate the configuration space. We have done this on the basis of excitation energy arguments. All $[qp\otimes 1ph]$ and $[qp\otimes 2ph]$ with $E_x\leqslant 6$ MeV, and $[qp\otimes 3ph]$ with $E_x\leqslant 8$ MeV configurations are included in the model space. The only exceptions are $[J_{\mathrm{g.s.}}\otimes 1^{-}]$ configurations which have not been truncated at all to treat a core polarization effect due to the coupling of low-energy dipole transitions to the GDR on a microscopic level. Thus, for electric dipole transitions we have no renormalized effective charges and used $e^{\mathrm{eff}}(p)=(N/A)\,e$ and $e^{\mathrm{eff}}(n)=-(Z/A)\,e$ values to separate the center of mass motion. For $M1$ transitions we use $g_s^{\mathrm{eff}}=0.64g_s^{\mathrm{free}}$ as recommended in Ref. [36]. By doing this all the important configurations for the description of low-lying states up to 4 MeV are included in the model space. The dimension of this space depends on the total spin of the excited states, and it varies between 500 and 700 configurations.

B. Comparison between experimental data and QPM calculations

Since only $E1$, $M1$, and $E2$ transitions can be observed in the present experiment, the discussion of the properties of the excited states will be restricted to states with $J^{\pi}=1/2^{\pm}$, $3/2^{\pm}$, and $5/2^{+}$. As the parities of the decaying levels are unknown and the spin could be assigned for only a few levels, the best quantity for the comparison between the theoretical predictions and the experimental results are the total integrated cross sections I_s. The theoretical reduced excitation probabilities $B(\pi L)\uparrow$ can be transformed into I_S values via the following relation:

$$I_S=\frac{8\pi^3(L+1)}{L[(2L+1)!!]^2}\left(\frac{E_x}{\hbar c}\right)^{2L-1}B(\pi L)\uparrow\frac{\Gamma_0}{\Gamma_{\mathrm{tot}}}, \tag{19}$$

where E_x is the excitation energy, L the multipolarity of the transition, and Γ_0 denotes the partial ground state decay

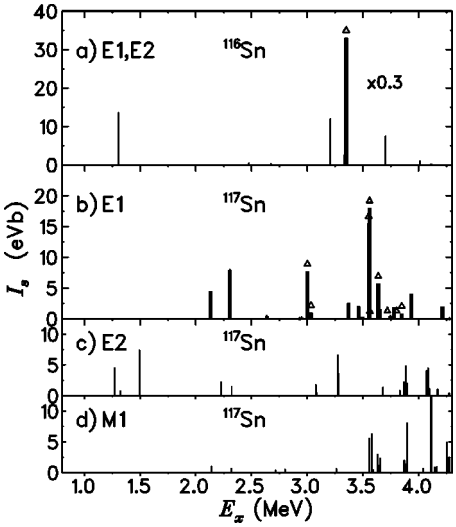

FIG. 5. Calculated integrated elastic photon scattering cross sections I_S in ^{116}Sn (a) and ^{117}Sn (b)–(d). The integrated cross sections I_S for $E1$ transitions are plotted by thick lines in (a) and (b). The $E1$ transitions in (b) which are predominantly due to $[3s_{1/2}\otimes[2_1^+\otimes 3_1^-]_{1^-}]_{1/2^-,3/2^-}\rightarrow 3s_{1/2}$ transitions are marked by triangles.

width. The obtained I_S values for the elastic transitions are plotted in Fig. 4(c) and compared with the results of our (γ,γ') experiments given in Fig. 4(b). The inelastic decays are accounted for in the total decay widths $\Gamma_{\rm tot}$. Details concerning the calculations and branching ratios will be discussed below. Supporting the experimental findings, our calculations also produce a strong fragmentation of the electromagnetic strength. The strongest transitions have $E1$ character, but also $E2$ and $M1$ excitations yield comparable cross sections. The total cross section I_S is disentangled into its $E1$, $M1$, and $E2$ components in Figs. 5(b)–5(d), and compared to the calculated I_s values of the core nucleus, ^{116}Sn [Fig. 5(a)]. The calculated sum of the total cross sections of the plotted $E1$, $M1$, and $E2$ transitions in Figs. 5(b)–5(d) equals 73, 37, and 42 eV b. The summed experimental elastic cross sections, shown in Fig. 4(b), equals 133 (21) eV b and agrees within 15% with the theoretically predicted value of 152 eV b.

Although the experimentally observed levels do not match in detail with the calculated level scheme one by one, some interesting general conclusions can be drawn. The most essential differences in the electromagnetic strength distribution over low-lying states in even-even ^{116,118}Sn and odd-mass ^{117}Sn take place for the electric dipole transitions. The reason becomes clear by considering which states can be excited from the ground state by $E1$ transitions. In the even-even core there is only one 1^- configuration with an excitation energy below 4 MeV [thick line with triangle in Fig. 5(a)]. It has a $[2_1^+\otimes 3_1^-]_{1^-}$ two-phonon nature [7]. This is a general feature in heavy semimagic even-even nuclei [8]. All other 1^- configurations have excitation energies more than 1 MeV higher. Therefore, the 1_1^- state has an almost pure two-phonon character in semimagic nuclei. In contrast, there are many $[qp\otimes 1ph]$ and $[qp\otimes 2ph]$ configurations with the same spin and parity close to the two corresponding configurations $[3s_{1/2}\otimes[2_1^+\otimes 3_1^-]_{1^-}]_{1/2^-,3/2^-}$ in ^{117}Sn. Interactions lead to a strong fragmentation of these two main configurations (see Table IV). The resulting states are carrying a fraction of the $E1$ excitation strength from the ground state.

TABLE IV. Theoretical excitation energies (E_x) and $B(E1)\downarrow$ reduced transition probabilities for decays into the $1/2_1^+$ ground state and the low-lying $3/2_1^+$ state for negative parity states in ^{117}Sn. Only the states with $B(E1,J^\pi\rightarrow 1/2_1^+)>10^{-5}$ e^2 fm^2 are presented. In the last two columns the contribution of the quasiparticle ($\alpha^+_{J^\pi}$) and the $[3s_{1/2}\otimes[2_1^+\otimes 3_1^-]_{1^-}]_{J^\pi}$ configurations to the wave functions of the states [see Eq. (9)] is provided if it is larger than 0.1%.

E_x (MeV)	$B(E1)\downarrow$ (10^{-3} e^2 fm^2) $J^\pi\rightarrow 1/2_1^+$	$J^\pi\rightarrow 3/2_1^+$	$\alpha^+_{J^\pi}$	$[\frac{1}{2}^+\otimes[2_1^+\otimes 3_1^-]_{1^-}]$
		$J^\pi=3/2^-$		
2.13	0.329	0.092	1.0%	
2.33	0.560	0.180	1.8%	
2.64	0.030	0.024		
3.04	0.058	0.032		10.7%
3.37	0.121	0.039	0.4%	
3.46	0.072	0.002	0.2%	
3.49	0.011	0.002		
3.55	0.551	0.012		47.8%
3.56	0.660	0.038	0.1%	32.0%
3.65	0.160	0.336	0.5%	0.1%
3.75	0.015	0.003		
3.78	0.081	0.033	0.3%	
3.85	0.042	0.025		2.8%
3.93	0.235	0.205	0.9%	
4.21	0.087	0.047	0.3%	
4.32	0.133	0.074	0.5%	
		$J^\pi=1/2^-$		
2.95	0.022	0.023		0.8%
3.00	0.698	0.072	0.1%	21.9%
3.63	0.560	0.250		62.9%
3.72	0.070	1.790		4.0%
4.45	0.020	0.005		

The predicted properties of some states with spin and parity $J^\pi=1/2^-$ and $3/2^-$ which can be excited from the $1/2^+$ ground state in ^{117}Sn by electric dipole transition are presented in Table IV. A large part of the $[3s_{1/2}\otimes[2_1^+\otimes 3_1^-]_{1^-}]_{1/2^-,3/2^-}$ configurations is concentrated in the $3/2^-$ states with an excitation energy of 3.04, 3.55, and 3.56 MeV and in the $1/2^-$ states at 3.00 and 3.63 MeV (see, fifth column of this table). These states are marked with triangles in Fig. 5(b) (as well as four other states with a smaller contribution of these configurations). The $E1$ strength distribution among low-lying levels is even more complex because $3/2^-$ states at 2.13, 2.33, and 3.93 MeV have a noticeable contribution from the $3p_{3/2}$ one-quasiparticle configuration (indicated in the fourth column of Table IV) with a large reduced excitation matrix element $\langle 3p_{3/2}||E1||3s_{1/2}\rangle$ for which there is no analogue in the even-even core ^{116}Sn. Also the coupling to $[3s_{1/2}\otimes 1^-_{\rm GDR}]$, which treats the core polarization effect, is somewhat different than in the core nucleus, be-

cause the blocking effect plays an important role in the interaction with other configurations (see also Ref. [34], where only the last type of transitions has been accounted for). The calculated total $B(E1)\uparrow$ strength in the energy region from 2.0 to 4.0 MeV is 7.2×10^{-3} $e^2\,\mathrm{fm}^2$. It agrees well with the calculated $B(E1,0^+_{\mathrm{g.s.}}\rightarrow[2^+\otimes3^-]_{1^-})=8.2\times10^{-3}$ $e^2\,\mathrm{fm}^2$ in the neighboring ^{116}Sn nucleus [7].

The calculations indicate that among the negative parity states in ^{117}Sn which are relatively strongly excited from the ground state, a few are characterized by a visible $E1$ decay into the low-lying $3/2^+_1$ state. These are $3/2^-$ states at 2.33, 3.65, and 3.93 MeV and $1/2^-$ state at 3.63 MeV. The state at 2.33 MeV decays into the $3/2^+_1$ state due to single-particle transition with a large reduced excitation matrix element $\langle 2d_{3/2}||E1||3p_{3/2}\rangle$. The states at higher energies decay into the $3/2^+_1$ state because of an admixture of $[3p_{1/2}\otimes[2^+_1\otimes3^-_1]_{1^-}]_{1/2^-,3/2^-}$ configurations in their wave functions.

Positive parity states in ^{117}Sn are deexciting to the $1/2^+$ ground state by $M1$ or $E2$ or mixed $M1/E2$ transitions. The predicted properties of the $1/2^+$, $3/2^+$, and $5/2^+$ states in ^{117}Sn are presented in Table V. The $B(E2)\uparrow$ strength distribution is dominated by the excitation of the $3/2^+$ state at 1.27 MeV and the $5/2^+$ state at 1.49 MeV. The wave functions of these states carry 85% and 60% of the $[3s_{1/2}\otimes2^+_1]$ configuration, respectively. These two states correspond with a high probability to the experimentally observed levels at 1447 and 1510 keV. A smaller fraction of the above mentioned configuration can be found in the $3/2^+$ state at 2.32 MeV (5%) and the $5/2^+$ state at 2.23 MeV (6%). The rather fragmented $E2$ strength at higher energies [Fig. 5(c)] is mainly due to $[3s_{1/2}\otimes2^+_{4,5}]$ configurations which are much less collective than the first one. Fragmented $E2$ strength between 2.0 and 4.0 MeV originating from the excitation of the $2^+_{4,5}$ phonons has also been observed in NRF experiments on the even-mass ^{116}Sn nucleus [37]. It could be well reproduced by theoretical calculations [see thin lines in Fig. 5(a)]. In the odd-mass ^{117}Sn nucleus the corresponding strength is even more fragmented because of the higher density of the configurations. Nevertheless, these $E2$ excitations at high energies contribute appreciably to the reaction cross section, because the $E2$ photon scattering cross section is a cubic function of the excitation energy [see Eq. (19)].

The $B(M1)\uparrow$ strength in the calculations is concentrated mainly above 3.5 MeV as can be seen in Fig. 5(d). The wave functions of the $1/2^+$ and $3/2^+$ states at these energies are very complex. The main configurations, responsible for the $M1$ strength, are the $[2d_{5/2,3/2}\otimes2^+_i]$ ones which are excited because of the internal fermion structure of the phonons (similar to $E1$ $0^+_{\mathrm{g.s.}}\rightarrow[2^+_1\otimes3^-_1]_{1^-}$ excitations). They have no analogous transitions in even-even nuclei. The configuration $[3s_{1/2}\otimes1^+_1]$ has an excitation energy of about 4.2 MeV but its contribution to the structure of states below 4 MeV is rather weak. Most of the states with the largest $B(M1)\uparrow$ values have $J^\pi=1/2^+$ (see Table V).

The QPM calculations show that the two-phonon $B(E1)$ strength from the even-even nuclei is fragmented over several states. Even with the present sensitivity of our NRF setup, it is impossible to resolve all of these details. Nevertheless, when all experimentally observed transitions between 2.7 and 3.6 MeV are considered to be $E1$ transitions, the total summed $B(E1)\uparrow$ strength amounts to 5.59 (64) 10^{-3} $e^2\,\mathrm{fm}^2$ or 85(13)–77(14) % of the two-phonon $B(E1)$ strength in the neighboring nuclei ^{116}Sn and ^{118}Sn. This value is considerably higher than in the case of ^{139}La and ^{141}Pr [17] where less than 40% was observed. It shows that the $1/2^+$ ground state spin of ^{117}Sn limits the possible fragmentation and hence a larger amount of the particle two-

TABLE V. Theoretical excitation energies (E_x) and $B(M1)\downarrow$ and $B(E2)\downarrow$ reduced transition probabilities for decays into the $1/2^+_1$ ground state and the low-lying $3/2^+_1$ states of positive parity states in ^{117}Sn. Only the states with $B(M1,J^\pi\rightarrow1/2^+_1)>10^{-2}$ μ_N^2 or $B(E2,J^\pi\rightarrow1/2^+_1)>1$ $e^2\,\mathrm{fm}^4$ are presented.

E_x	$B(M1)\downarrow$ (μ_N^2)		$B(E2)\downarrow$ ($e^2\,\mathrm{fm}^4$)	
MeV	$J^\pi\rightarrow1/2^+_1$	$J^\pi\rightarrow3/2^+_1$	$J^\pi\rightarrow1/2^+_1$	$J^\pi\rightarrow3/2^+_1$
		$J^\pi=1/2^+$		
2.14	0.011	0.001		
3.58	0.039	0.006		
3.66	0.010	0.014		
3.87	0.012	0.002		
3.89	0.035	0.012		
4.02	0.045	0.031		
4.10	0.200			
4.25	0.027			
		$J^\pi=3/2^+$		
1.27			353	1
1.39			1	353
1.78		0.005	2	7
2.32	0.003		20	12
2.47			2	10
3.07			10	
3.28			16	
3.56	0.018	0.009		1
3.63	0.010	0.040		
3.66	0.001	0.004	5	
3.87		0.001	8	2
3.88	0.002		4	1
4.05	0.002		10	
4.17			1	
4.42	0.011	0.004		
		$J^\pi=5/2^+$		
1.01			82	11
1.32			37	309
1.49			239	25
2.22			1	4
2.23			22	1
3.07			2	1
3.27			20	
3.79			2	
3.87			4	
3.89			8	
4.06			9	
4.17			1	

phonon coupled $B(E1)$ strength could be resolved in this NRF experiment.

V. CONCLUSIONS

Nuclear resonance fluorescence experiments performed on the odd-mass spherical nucleus ^{117}Sn revealed a large fragmentation of the electromagnetic strength below an excitation energy of 4 MeV. The search for the fragments of the $3s_{1/2} \otimes [2_1^+ \otimes 3_1^-]$ multiplet carrying the $B(E1)$ strength of the adjacent even-even nuclei is complicated by the limited spin information. QPM calculations carried out for the first time in a complete configuration space can explain the fragmentation of the excitation strength and shed light on how the $B(E1)$, $B(M1)$, and $B(E2)$ strength is distributed over this energy region.

ACKNOWLEDGMENTS

This work is part of the research program of the Fund for Scientific Research Flanders. The support by the Deutsche Forschungsgemeinschaft (DFG) under Contract Nos. Kn 154-30 and Br 799/9-1 is gratefully acknowledged. V.Yu.P. acknowledges financial support from the Research Council of the University of Gent and NATO.

[1] U. Kneissl, H. H. Pitz, and A. Zilges, Prog. Part. Nucl. Phys. **37**, 349 (1996).

[2] A. Zilges, P. von Brentano, H. Friedrichs, R. D. Heil, U. Kneissl, S. Lindenstruth, H. H. Pitz, and C. Wesselborg, Z. Phys. A **340**, 155 (1991).

[3] U. Kneissl, A. Zilges, J. Margraf, I. Bauske, P. von Brentano, H. Friedrichs, R. D. Heil, R.-D. Herzberg, H. H. Pitz, B. Schlitt, and C. Wesselborg, Phys. Rev. Lett. **71**, 2180 (1993).

[4] C. Fransen, O. Beck, P. von Brentano, T. Eckert, R.-D. Herzberg, U. Kneissl, H. Maser, A. Nord, N. Pietralla, H. H. Pitz, and A. Zilges, Phys. Rev. C **57**, 129 (1998).

[5] R.-D. Herzberg, I. Bauske, P. von Brentano, Th. Eckert, R. Fischer, W. Geiger, U. Kneissl, J. Margraf, H. Maser, N. Pietralla, H. H. Pitz, and A. Zilges, Nucl. Phys. **A592**, 211 (1995).

[6] K. Govaert, L. Govor, E. Jacobs, D. De Frenne, W. Mondelaers, K. Persyn, M.-L. Yoneama, U. Kneissl, J. Margraf, H. H. Pitz, K. Huber, S. Lindenstruth, R. Stock, K. Heyde, A. Vdovin, and V. Yu. Ponomarev, Phys. Lett. B **335**, 113 (1994).

[7] J. Bryssinck, L. Govor, D. Belic, F. Bauwens, O. Beck, P. von Brentano, D. De Frenne, T. Eckert; C. Fransen, K. Govaert, R.-D. Herzberg, E. Jacobs, U. Kneissl, H. Maser, A. Nord, N. Pietralla, H. H. Pitz, V. Yu. Ponomarev, and V. Werner, Phys. Rev. C **59**, 1930 (1999).

[8] V. Yu. Ponomarev, Ch. Stoyanov, N. Tsoneva, and M. Grinberg, Nucl. Phys. **A635**, 470 (1998).

[9] R. A. Gatenby, J.R. Vanhoy, E. M. Baum, E. L. Johson, S.W. Yates, T. Belgya, B. Fazekas, A. Veres, and G. Molnár, Phys. Rev. C **41**, R414 (1990).

[10] S. J. Robinson, J. Jolie, H. G. Börner, P. Schillebeeckx, S. Ulbig, and K. P. Lieb, Phys. Rev. Lett. **73**, 412 (1994).

[11] T. Belgya, R. A. Gatenby, E. M. Baum, E. L. Johnson, D. P. DiPrete, S. W. Yates, B. Fazekas, and G. Molnár, Phys. Rev. C **52**, R2314 (1995).

[12] M. Wilhelm, E. Radermacher, A. Zilges, and P. von Brentano, Phys. Rev. C **54**, R449 (1996).

[13] M. Wilhelm, S. Kasemann, G. Pacovici, E. Radermacher, P. von Brentano, and A. Zilges, Phys. Rev. C **57**, 577 (1998).

[14] P. E. Garrett, H. Lehmann, J. Jolie, C. A. McGrath, Minfang Yeh, and S. W. Yates, Phys. Rev. C **59**, 2455 (1999).

[15] A. Zilges, R.-D. Herzberg, P. von Brentano, F. Dönau, R. D. Heil, R. V. Jolos, U. Kneissl, J. Margraf, H. H. Pitz, and C. Wesselborg, Phys. Rev. Lett. **70**, 2880 (1993).

[16] R.-D. Herzberg, A. Zilges, A. M. Oros, P. von Brentano, U. Kneissl, J. Margraf, H. H. Pitz, and C. Wesselborg, Phys. Rev. C **51**, 1226 (1995).

[17] R.-D. Herzberg, I. Bauske, O. Beck, P. von Brentano, T. Eckert, R. Fischer, D. Jäger, U. Kneissl, J. Margraf, H. Maser, H. H. Pitz, M. Rittner, A. Schiller, and A. Zilges, in *Proceedings of the XII International School on Nuclear Physics, Neutron Physics and Nuclear Energy, Varna, Bulgaria*, edited by W. Andrejtscheff and D. Elenkov (Institute for Nuclear Research and Nuclear Energy, Sofia, Bulgaria, 1995), p. 165.

[18] W. Geiger, Zs. Németh, I. Bauske, P. von Brentano, R. D. Heil, R.-D. Herzberg, U. Kneissl, J. Margraf, H. Maser, N. Pietralla, H. H. Pitz, C. Wesselborg, and A. Zilges, Nucl. Phys. **A520**, 263 (1994).

[19] J. Besserer, O. Beck, P. von Brentano, T. Eckert, R.-D. Herzberg, D. Jäger, U. Kneissl, J. Margraf, H. Maser, A. Nord, N. Pietralla, H.H. Pitz, and A. Zilges, Phys. Rev. C **56**, 1276 (1997).

[20] V. Yu. Ponomarev, J. Bryssinck, L. Govor, F. Bauwens, O. Beck, D. Belic, P. von Brentano, D. De Frenne, C. Fransen, R.-D. Herzberg, E. Jacobs, U. Kneissl, H. Maser, A. Nord, N. Pietralla, H. H. Pitz, and V. Werner, Phys. Rev. Lett. **83**, 4029 (1999).

[21] F. R. Metzger, Prog. Nucl. Phys. **7**, 53 (1959).

[22] S. J. Skorka, in *The Electromagnetic Interaction in Nuclear Spectroscopy*, edited by W. D. Hamilton (North-Holland, Amsterdam, 1975).

[23] N. Pietralla, I. Bauske, O. Beck, P. von Brentano, W. Geiger, R.-D. Herzberg, U. Kneissl, J. Margraf, H. Maser, H. H. Pitz, and A. Zilges, Phys. Rev. C **51**, 1021 (1995).

[24] B. Schlitt, U. Maier, H. Friedrichs, S. Albers, I. Bauske, P. von Brentano, R. D. Heil, R.-D. Herzberg, U. Kneissl, J. Margraf, H. H. Pitz, C. Wesselborg, and A. Zilges, Nucl. Instrum. Methods Phys. Res. A **337**, 416 (1994).

[25] U. E. P. Berg and U. Kneissl, Annu. Rev. Nucl. Part. Sci. **37**, 33 (1987).

[26] K. Govaert, W. Mondelaers, E. Jacobs, D. De Frenne, K. Persyn, S. Pomme, M.-L. Yoneama, S. Lindenstruth, K. Huber, A. Jung, B. Starck, R. Stock, C. Wesselborg, R.-D. Heil, U. Kneissl, and H. H. Pitz, Nucl. Instrum. Methods Phys. Res. A **337**, 265 (1994).

[27] J. Blachot and G. Marguier, Nucl. Data Sheets **50**, 101 (1987).
[28] V. G. Soloviev, *Theory of Atomic Nuclei: Quasiparticles and Phonons* (IOP, Bristol and Philadelphia, 1992).
[29] A. I. Vdovin, V. V. Voronov, V. G. Soloviev, and Ch. Stoyanov, Part. Nuclei **16**, 245 (1985).
[30] S. Gales, Ch. Stoyanov, and A. I. Vdovin, Phys. Rep. **166**, 125 (1988).
[31] V. Yu. Ponomarev, A. P. Dubensky, V. P. Dubensky, and E. A. Boiykova, J. Phys. G **16**, 1727 (1990).
[32] M. Huber, P. von Neumann-Cosel, A. Richter, C. Schlegel, R. Schultz, J. J. Carroll, K. N. Taylor, D. G. Richmond, T. W. Sinor, C. B. Collins, and V. Yu. Ponomarev, Nucl. Phys. **A559**, 253 (1993).
[33] J. J. Carroll, C. B. Collins, K. Heyde, M. Huber, P. von Neumann-Cosel, V. Yu Ponomarev, D. G. Richmond, A. Richter, C. Schlegel, T. W. Sinor, and K. N. Taylor, Phys. Rev. C **48**, 2238 (1993).
[34] P. von Neumann-Cosel, V. Yu. Ponomarev, A. Richter, and C. Spieler, Z. Phys. A **350**, 303 (1995).
[35] C. A. Bertulani and V. Yu. Ponomarev, Phys. Rep. **321**, 139 (1999).
[36] P. von Neumann-Cosel, F. Neumeyer, S. Nishizaki, V. Yu. Ponomarev, C. Rangacharyulu, B. Beitz, A. Richter, G. Schrieder, D. I. Sober, T. Waindzoch, and J. Wambach, Phys. Rev. Lett. **82**, 1105 (1999).
[37] J. Bryssinck, L. Govor, V. Yu. Ponomarev, D. Belic, F. Bauwens, O. Beck, P. von Brentano, D. De Frenne, T. Eckert, C. Fransen, K. Govaert, R.-D. Herzberg, E. Jacobs, U. Kneissl, H. Maser, A. Nord, N. Pietralla, H.H. Pitz, and V. Werner, Phys. Rev. C **61**, 024309 (2000).